Information-Length Scaling in a Generalized One-Dimensional Lloyd's Model

J. A. Méndez-Bermúdez [1],* (ID) **and R. Aguilar-Sánchez [2]**

[1]   Instituto de Física, Benemérita Universidad Autónoma de Puebla, Puebla 72570, Mexico
[2]   Facultad de Ciencias Químicas, Benemérita Universidad Autónoma de Puebla, Puebla 72570, Mexico; ras747698@gmail.com
*   Correspondence: jmendezb@ifuap.buap.mx; Tel.: +52-222-229-5610

Abstract: We perform a detailed numerical study of the localization properties of the eigenfunctions of one-dimensional (1D) tight-binding wires with on-site disorder characterized by long-tailed distributions: For large ϵ, $P(\epsilon) \sim 1/\epsilon^{1+\alpha}$ with $\alpha \in (0,2]$; where ϵ are the on-site random energies. Our model serves as a generalization of 1D Lloyd's model, which corresponds to $\alpha = 1$. In particular, we demonstrate that the information length β of the eigenfunctions follows the scaling law $\beta = \gamma x/(1 + \gamma x)$, with $x = \xi/L$ and $\gamma \equiv \gamma(\alpha)$. Here, ξ is the eigenfunction localization length (that we extract from the scaling of Landauer's conductance) and L is the wire length. We also report that for $\alpha = 2$ the properties of the 1D Anderson model are effectively reproduced.

Keywords: Lloyd model; scaling laws; information length; one-dimensional disordered systems

1. Introduction

There is a class of disordered systems characterized by random variables $\{\epsilon\}$ whose density distribution function exhibits a slow decaying tail:

$$P(\epsilon) \sim \frac{1}{|\epsilon|^{1+\alpha}} \, , \tag{1}$$

for large $|\epsilon|$, with $0 < \alpha < 2$. The study of this class of disordered systems dates back to Lloyd [1], who studied spectral properties of a three-dimensional (3D) lattice described by a 3D tight-binding Hamiltonian with Cauchy-distributed on-site potentials (which corresponds to the particular value $\alpha = 1$ in Equation (1)). Since then, a considerable number of works have been devoted to the study of spectral, eigenfunction, and transport properties of Lloyd's model in its original 3D setup [2–12] and in lower dimensional versions [11–30]. Consequently, disorder characterized by Equation (1) is commonly known as Lévy-type disorder. In addition, the recent experimental realizations of the so-called Lévy glasses [31] as well as Lévy waveguides [32,33] has refreshed the interest in the study of systems characterized by Lévy-type disorder; see some examples in Refs. [34–50].

It is important to point out that one-dimensional (1D) tight-binding wires with power-law distributed random on-site potentials, characterized by power-laws different from $\alpha = 1$ (which corresponds to the 1D Lloyd's model), have been scarcely studied; for prominent exceptions see Refs. [26,27]. Thus, in this paper, we perform a detailed numerical study of the localization properties of the eigenfunctions of disordered wires defined as a generalization of the 1D Lloyd's model as follows. We shall study 1D wires described by the Hamiltonian

$$H = \sum_{n=1}^{L} \left[\epsilon_n \mid n \rangle \langle n \mid - v_{n,n+1} \mid n \rangle \langle n+1 \mid - v_{n,n-1} \mid n \rangle \langle n-1 \mid \right]; \tag{2}$$

where L is the length of the wire given as the total number of sites n, ϵ_n are random on-site potentials, and $v_{n,m}$ are the hopping integrals between nearest neighbours. In particular, we set $v_{n,m} = v = 1$ and consider the on-site potentials ϵ_n following the distribution of Equation (1) with $0 < \alpha \leq 2$. We note that when $\alpha = 1$ we recover the original 1D Lloyd's model.

Of particular interest is the comparison between the 1D Anderson model [51] and our generalization of 1D Lloyd's model, since the former represents the most prominent model of disordered wires [52]. Indeed, the 1D Anderson model is also described by the tight-binding Hamiltonian of Equation (2). However, while for the standard 1D Anderson model (with white-noise on-site disorder $\langle \epsilon_n \epsilon_m \rangle = \sigma^2 \delta_{nm}$ and $\langle \epsilon_n \rangle = 0$) the on-site potentials are characterized by a finite variance $\sigma^2 = \langle \epsilon_n^2 \rangle$ (in most cases the corresponding probability distribution function $P(\epsilon)$ is chosen as a box or a Gaussian distribution), in the generalized 1D Lloyd's model the second moment of the random on-site energies ϵ_n diverges for $0 < \alpha < 2$, and if $0 < \alpha < 1$ also the first moment diverges. Moreover, when $\alpha = 2$ the properties of the generalized 1D Lloyd's model are expected to be similar to those of the 1D Anderson model, since the variance of Equation (1) becomes finite.

It is relevant to recall that the eigenstates Ψ of the *infinite* 1D Anderson model are exponentially localized around a site position n_0 [52]:

$$|\Psi_n| \sim \exp\left(-\frac{|n - n_0|}{\xi}\right) \; ; \tag{3}$$

where ξ is the eigenfunction localization length. Moreover, for weak disorder ($\sigma^2 \ll 1$), the only relevant parameter for describing the statistical properties of the transmission of the *finite* 1D Anderson model is the ratio L/ξ [53], a fact known as single parameter scaling. The above exponential localization of eigenfunctions strongly affects the scattering and transport properties of the corresponding open wire. In particular, the transmission or dimensionless conductance G, that within a scattering approach to the electronic transport is given as [54–57]

$$G = |t|^2 \tag{4}$$

(where t is the transmission amplitude of the 1D wire), becomes exponentially small [58]:

$$\langle -\ln G \rangle = \frac{2}{x} \tag{5}$$

with

$$x = \frac{\xi}{L} \; . \tag{6}$$

Thus, relation (5) can be used to obtain the localization length ξ from the transmission of the disordered wire. Remarkably, it has been shown that Equation (5) is also valid for the generalized 1D Lloyd's model [26,27] implying the single parameter scaling, see also [22,23].

Moreover, outstandingly, it has been found [30] that the eigenfunction properties of both the 1D Anderson model and the 1D Lloyd's model (i.e., our generalized 1D Lloyd's model with $\alpha = 1$), characterized by the *information length* β (defined in Equation (12) below), are *universal* for the fixed ratio of Equation (6). More specifically, it was numerically shown that the scaling function

$$\beta = \frac{\gamma x}{1 + \gamma x} \; , \tag{7}$$

with $\gamma \sim 1$, holds; see also [59].

Thus, below we explore the validity of scaling (7) for the eigenfunctions of the generalized 1D Lloyd's model. Of particular relevance is the regime $0 < \alpha < 1$ where the coexistence of insulating and ballistic regimes has been reported [27] (evidenced by well defined peaks in $P(G)$ at $G = 0$ and

$G = 1$); a signature of the coexistence of localized and extended eigenfunctions. In our study, we use the 1D Anderson model as reference.

Alongside this work we generate the random variables $\{\epsilon\}$ needed to construct the generalized 1D Lloyd's model by the use of the algorithm introduced in Ref. [60]. That algorithm was designed to produce random variables having the probability density function

$$\mathcal{P}(\epsilon) = \frac{\mathcal{C}}{\epsilon^{1+\alpha}} \, , \tag{8}$$

which has a lower cut-off at $\epsilon_0 = (\mathcal{C}/\alpha)^{1/\alpha}$ such that $\int_{\epsilon_0}^{\infty} \mathcal{P}(\epsilon)d\epsilon = 1$. In addition, we randomize the signs of the obtained variables $\{\epsilon\}$ in order to set the band center of the generalized 1D Lloyd's model to $E = 0$. Moreover, we have verified that our conclusions do not depend on our choice of $\mathcal{P}(\epsilon)$. Indeed, we obtained similar results (not shown here) with $\mathcal{P}(\epsilon) = \alpha/(1+\epsilon)^{1+\alpha}$ and $\mathcal{P}(\epsilon) = [1/\Gamma(\alpha)]2^{-\alpha}\exp(-1/2\epsilon)/\epsilon^{1+\alpha}$ (where Γ is the Euler gamma function), that we also used in [27].

2. Results

2.1. Extraction of the Localization Length ξ

We obtain the localization length ξ for the generalized 1D Lloyd's model as follows: We open the isolated wires by attaching two semi-infinite single channel leads to the border sites at opposite sides. Each lead is described by a 1D semi-infinite tight-binding Hamiltonian. Using standard methods, see e.g., [61–64], we can write the transmission amplitude through the disordered wires as

$$t = -2i\sin(k)\,\mathcal{W}^T \frac{1}{E - \mathcal{H}_{\text{eff}}} \mathcal{W} \, , \tag{9}$$

where $k = \arccos(E/2)$ is the wave vector supported in the leads and $\mathcal{H}_{\text{eff}}$ is an effective non-hermitian Hamiltonian given by $\mathcal{H}_{\text{eff}} = H - e^{ik}\mathcal{W}\mathcal{W}^T$. Here, $\mathcal{W}$ is a $L \times 1$ vector that specifies the positions of the attached leads to the wire. In our setup, all elements of $\mathcal{W}$ are equal to zero except $\mathcal{W}_{11}$ and $\mathcal{W}_{L1}$ which we set to unity (i.e., the leads are attached to the wire with a strength equal to the inter-site hopping amplitudes: $v = 1$). Also, we have fixed the energy at $E = 0$. Therefore, we use Equation (4) to compute G.

Then, in Figure 1a we present the ensemble average $\langle -\ln G \rangle$ as a function of L for the generalized 1D Lloyd's model for several values of α. It is clear from this figure that $\langle -\ln G \rangle \propto L$ for all the values of α we consider here. Therefore, we can extract the localization length ξ by fitting the curves $\langle -\ln G \rangle$ vs. L with Equation (5); see dashed lines in Figure 1a. We have observed that it is possible to tune ξ for the same value of α by moving $\mathcal{C}$ in Equation (8). Thus, in Figure 1b we report the values of ξ, extracted from the curves $\langle -\ln G \rangle$ vs. L, as a function of $\mathcal{C}$. Moreover, note that

$$\xi \propto \mathcal{C}^{-\alpha} \, , \tag{10}$$

as shown with the dashed lines in Figure 1b.

In the following Subsection, we use the values of ξ obtained here to construct the ratio of Equation (6) and verify scaling (7) accordingly.
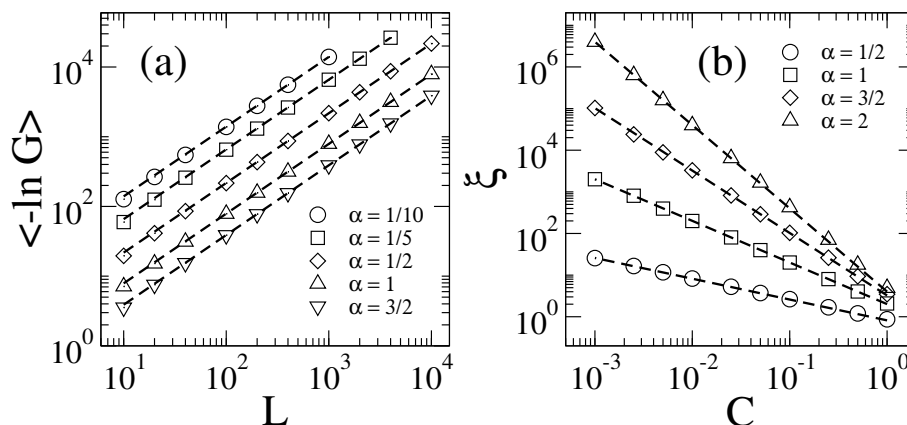
Figure 1. (**a**) Average logarithm of the conductance $\langle -\ln G \rangle$ as a function of L for the generalized 1D Lloyd's model characterized by the values of α indicated on the figure (symbols). $\mathcal{C} = 1$ and $E = 0$ were used. Each point was calculated using 10^4 disorder realizations. Dashed lines are the fittings of the data with Equation (5). The obtained values of ξ from the fittings are: $\xi \approx 0.143$ (for $\alpha = 1/10$), $\xi \approx 0.304$ (for $\alpha = 1/5$), $\xi \approx 0.919$ (for $\alpha = 1/2$), $\xi \approx 2.535$ (for $\alpha = 1$), and $\xi \approx 5.144$ (for $\alpha = 3/2$). (**b**) ξ as a function of the constant $\mathcal{C}$. Dashed lines are the fittings of the data with Equation (10). The obtained values for the proportionality constant c from the fittings are: $c \approx 0.82$ (for $\alpha = 1/2$), $c \approx 2.01$ (for $\alpha = 1$), $c \approx 3.25$ (for $\alpha = 3/2$), and $c \approx 4.01$ (for $\alpha = 2$). Error bars on both panels are not shown since they are much smaller than symbol size.

2.2. Calculation of the Information Length β

We compute the information length β for the generalized 1D Lloyd's model by the use of the Shannon entropy S of the corresponding eigenfunctions: With the Shannon entropy for the eigenfunction Ψ^m, which is given as

$$S = -\sum_{n=1}^{L} (\Psi_n^m)^2 \ln(\Psi_n^m)^2 , \tag{11}$$

we write β (see e.g., [65]) as

$$\beta = \exp\left[-\left(S_{\text{GOE}} - \langle S \rangle\right)\right] . \tag{12}$$

Here $S_{\text{GOE}} \approx \ln(L/2.07)$ is the entropy of a random eigenfunction with Gaussian distributed amplitudes (i.e., an eigenfunction of the Gaussian Orthogonal Ensemble [66]). With this definition for S (recall that S provides the number of principal components of an eigenfunction in a given basis) and β, when the eigenfunctions are localized $\langle S \rangle \approx 0$ and $\beta \approx 2.07/L$, which tends to zero for large L. On the other hand, when *fully chaotic* eigenfunctions extend over the L available basis states $\langle S \rangle = S_{\text{GOE}}$ and $\beta = 1$. Therefore, β can take values in the range $(0, 1]$.

Below we use exact numerical diagonalization to obtain the eigenfunctions Ψ^m ($m = 1 \ldots L$) of large ensembles of the generalized 1D Lloyd's model characterized by the parameters L, $\mathcal{C}$, and α. We perform the average $\langle S \rangle$ taking half of the eigenfunctions, around the band center, for each disordered wire length such that $\langle S \rangle$ is computed with 10^5 data values. For example, since for a wire of length $L = 10^3$ we extract $10^3/2$ Shannon entropies only, we construct an ensemble of 2×10^2 disordered wires of that length to compute $\langle S \rangle$ from a double average; that is, we average over a subset of the eigenfunctions and over wire realizations. We use half of the eigenfunctions around the band center to be consistent with the fact that we have fixed $E = 0$ in Equation (9), however we have verified that our conclusions do not depend on this choice: i.e., we could reduce the energy window around $E = 0$ or even consider all eigenfunctions to compute $\langle S \rangle$ obtaining equivalent results.

In Figure 2a we present β as a function of ξ/L, see Equations (6) and (7), for the generalized 1D Lloyd's model with $\alpha = 1$, i.e., for the actual 1D Lloyd's model. Recall that to construct the ratios

ξ/L we are using the values of ξ obtained in the previous Subsection from the scaling of Landauer's conductance; see Figure 1a. In addition, in Figure 2b the logarithm of $\beta/(1-\beta)$ as a function of $\ln(\xi/L)$ is presented. The quantity $\beta/(1-\beta)$ is useful in the study of the scaling properties of β because

$$\frac{\beta}{1-\beta} = \gamma x \,, \tag{13}$$

which is obtained directly by equating γx from (7), implies that a plot of $\ln[\beta/(1-\beta)]$ vs. $\ln(x)$ (with $x = \xi/L$) is a straight line with unit slope. This fact applies for 1D Lloyd's model as can be easily verified by comparing the black symbols with the black dashed line in Figure 2b. Note that to construct Figure 2 we have used wires with lengths in the range $10^2 \le L \le 10^3$ only, however by changing $\mathcal{C}$ (different symbols indicate different values of $\mathcal{C}$) it is possible to span a large range of ξ/L values.
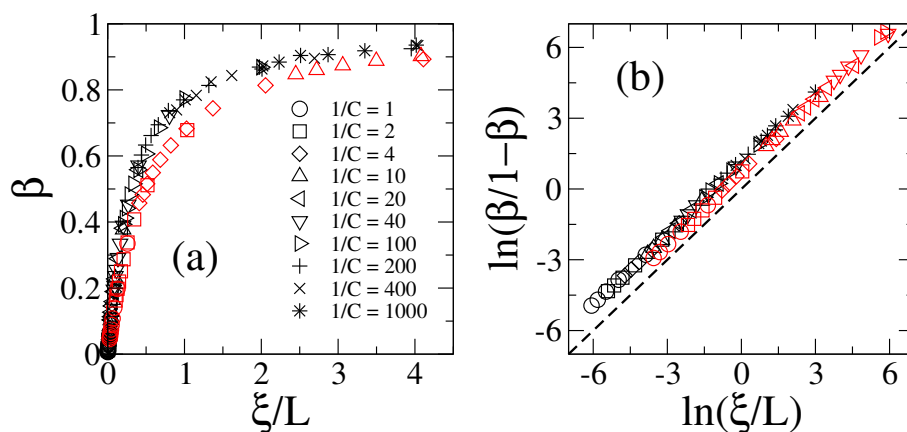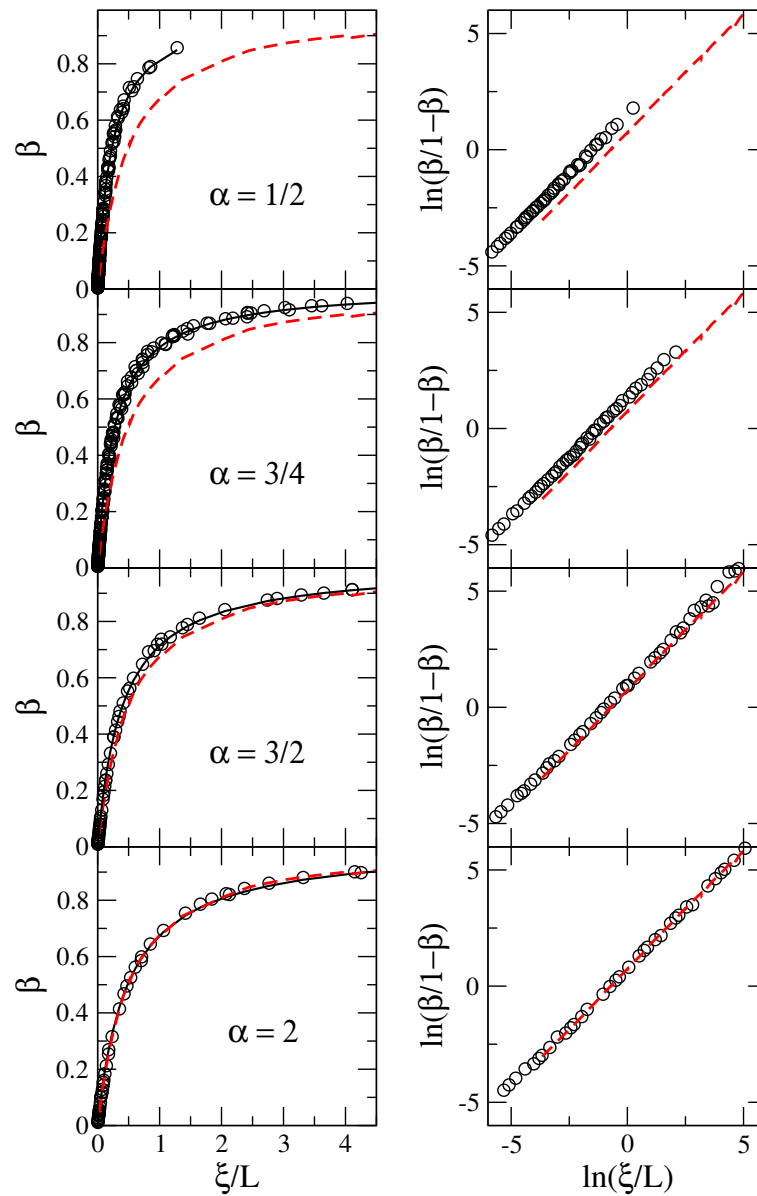

Figure 2. (**a**) Information length β as a function of ξ/L [see Equations (6) and (7)] for the generalized 1D Lloyd's model with $\alpha = 1$ (black symbols) and the 1D Anderson model (red symbols). (**b**) Logarithm of $\beta/(1-\beta)$ as a function of $\ln(\xi/L)$ [see Equation (13)]. Different symbols correspond to disorder distributions with different constants $\mathcal{C}$, as indicated in (**a**). Each symbol is computed by averaging over 10^5 eigenstates. Wires with $10^2 \le L \le 10^3$ were used. The identity, black dashed line in (**b**), is shown to guide the eye.

In Figure 2 we include, in red symbols, the corresponding data for the 1D Anderson model. Note that the functional forms in both panels, for both data sets, are very similar. With this, we confirm that scaling (7) is valid for the 1D Lloyd's model and the 1D Anderson model; as already shown in [30].

Now, in Figure 3 we plot curves of β vs. ξ/L (left panels) and $\ln[\beta/(1-\beta)]$ vs. $\ln(\xi/L)$ (right panels) for several values of α. Again, as reference, we include curves for the 1D Anderson model (red dashed lines). In particular, we present representative values of α in the interval $0 < \alpha < 1$ ($\alpha = 1/2$ and $3/4$), one value of α in the interval $1 \le \alpha < 2$ ($\alpha = 3/2$), and $\alpha = 2$. We stress the choice of the values of α in Figure 3 because it is known that the properties of systems with Levy-type disorder can be significantly different when the disorder is characterized by values of α in the intervals $0 < \alpha < 1$ or $1 \le \alpha < 2$. However, as shown in Figure 3 there is no major difference between different values of α except for the evolution of the curves towards that for the 1D Anderson model when increasing α. In fact, once $\alpha = 2$ the 1D Anderson model is effectively reproduced, see the lower panels of Figure 3.

Thus, we have verified that scaling (7) describes remarkably well all data sets. Indeed, in left panels of Figure 3 we show fittings of the data with Equation (7); see full black lines. Finally, in Figure 4 we report the values of the coefficients γ, obtained from the fittings of the data using Equation (7), for the values of α considered here. Clearly, when $\alpha = 2$, the coefficient γ is already very close to that for the 1D Anderson model ($\gamma \approx 2$); while, in the opposite limit (i.e., when $\alpha \to 0$) the value of γ becomes relatively large.

Figure 3. (**Left panels**) Information length β as a function of ξ/L [see Equations (6) and (7)] for ensembles of 1D disordered wires. (**Right panels**) Logarithm of $\beta/(1-\beta)$ as a function of $\ln(\xi/L)$ [see Equation (13)]. Black circles correspond to the generalized 1D Lloyd's model with $\alpha = 1/2$, 3/4, 3/2, and 2 (from top to bottom); while the Anderson model is represented by red dashed lines. Each symbol is computed by averaging over 10^5 (10^6) eigenstates when $L \geq 10^2$ ($L < 10^2$). Here, as in Figure 2, we change $\mathcal{C}$ to span a large range of ξ/L values however we do not use different symbols to indicate different values of $\mathcal{C}$ to avoid figure saturation. Full black lines in left panels correspond to fittings of the data with Equation (7) with $\gamma \approx 4.3798$ (for $\alpha = 1/2$), $\gamma \approx 3.5453$ (for $\alpha = 3/4$), $\gamma \approx 2.4891$ (for $\alpha = 3/2$), and $\gamma \approx 2.069$ (for $\alpha = 2$).
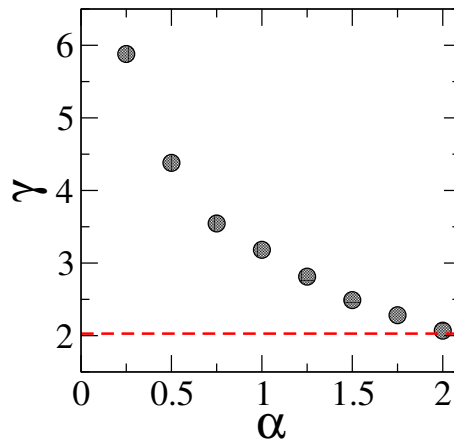
Figure 4. Coefficient γ as a function of α, obtained from the fittings of the curves β vs. ξ/L with Equation (7); see left panels in Figure 3. Black circles correspond to the generalized 1D Lloyd's model, while the 1D Anderson model is represented by the red dashed line at $\gamma \approx 2$. Error bars are not shown since they are much smaller than symbol size.

3. Discussion

In this paper, by the use of extensive numerical simulations, we demonstrate that the information length β of the eigenfunctions of our generalization of 1D Lloyd's model scales with the ratio $x = \xi(\alpha)/L$ as $\gamma x/(1 + \gamma x)$, where $\xi(\alpha)$ is the eigenfunction localization length, $\gamma \equiv \gamma(\alpha)$, and L is the wire length. Here α is the power-law decay of the long-tailed distributions, $P(\epsilon) \sim 1/\epsilon^{1+\alpha}$, characterizing the on-site random energies of 1D tight-binding wires.

It is particularly relevant that scaling (7) describes the eigenfunction properties of our generalization of 1D Lloyd's model for all values of α, since it has been shown that transport properties of this model are significatively different in the intervals $0 < \alpha < 1$ and $1 \leq \alpha < 2$ [27]. Moreover, we have shown that for $\alpha = 2$ the generalized 1D Lloyd's model already reproduces the properties of the 1D Anderson model.

It is pertinent to add that scaling (7) is also valid for the eigenfunctions of other disordered models (when the scaling parameter x is properly defined): the banded random matrix (BRM) model [67–74], the kicked-rotator model [65,71,75] (a quantum-chaotic system characterized by a random-like banded Hamiltonian matrix), the diluted BRM model [76], and multiplex and multilayer random networks [77]. Thus, we include our generalization of 1D Lloyd's model to the family of complex systems described by scaling (7).

Finally, we want to recall that scaling (7), can be rewritten in a "model independent" form as a relation between properly-defined inverse lengths [30,67]:

$$\frac{1}{d(L,\xi)} = \frac{1}{d(\infty,\xi)} + \frac{1}{d(L,0)} \, , \tag{14}$$

were $d(L,\xi) \equiv \exp[\langle S(L,\xi) \rangle]$, which is also applicable to our generalization of 1D Lloyd's model.

Author Contributions: The authors contributed equally to this work. J. A. Mendez-Bermudez and R. Aguilar-Sanchez conceived, designed and performed the experiments; J. A. Mendez-Bermudez and R. Aguilar-Sanchez analyzed the data and wrote the paper.

Conflicts of Interest: The authors declare no conflict of interest.

References

1. Lloyd, P. Exactly solvable model of electronic states in a three-dimensional disordered Hamiltonian: non-existence of localized states. *J. Phys. C* **1969**, *2*, 1717–1725. [CrossRef]

2. Saitoh, M. Existence of localization in Lloyd's disordered lattice model. *Phys. Lett. A* **1970**, *33*, 44–45. [CrossRef]

3. Saitoh, M. Electric Conductivity for Lloyd's Disordered Lattice Model. *Progr. Theor. Phys.* **1971**, *45*, 746–755. [CrossRef]

4. Kumar, A.P.; Baskaran, G. Coherent potential approximation, averaged T-matrix approximation and Lloyd's model. *J. Phys. C* **1973**, *6*, L399–L401. [CrossRef]

5. Hoshino, K. Electrical conductivity and electron localization for the Lloyd model. *Phys. Lett. A* **1976**, *56*, 133–134. [CrossRef]

6. Bandy, W.R.; Glick, A.J. Tight-binding Green's-function calculations of electron tunneling. II. Diagonal disorder in the one-dimensional two-band model. *Phys. Rev. B* **1977**, *16*, 2346–2349. [CrossRef]

7. Kivelson, S.; Gelatt, C.D. Impurity states in a disordered insulator: The Lloyd model. *Phys. Rev. B* **1979**, *20*, 4167–4170. [CrossRef]

8. Simon, B. Equality of the density of states in a wide class of tight-binding Lorentzian random models. *Phys. Rev. B* **1983**, *27*, 3859–3860. [CrossRef]

9. Rodrigues, D.E.; Weisz, J.F. Generalization of the Lloyd model for calculation of electronic structure at disordered interfaces. *Phys. Rev. B* **1986**, *34*, 2306–2310. [CrossRef]

10. Kolley, E.; Kolley, W. Conductivity in Anderson-type models: a comparative study of critical disorder. *J. Phys. C* **1988**, *21*, 6099–6109. [CrossRef]

11. Johnston, R.; Kunz, H. A method for calculating the localisation length, with an analysis of the Lloyd model. *J. Phys. C* **1983**, *16*, 4565–4580. [CrossRef]

12. Rodrigues, D.E.; Pastawski, H.M.; Weisz, J.F. Localization and phase coherence length in the Lloyd model. *Phys. Rev. B* **1986**, *34*, 8545–8549. [CrossRef]

13. Thouless, D.J. A relation between the density of states and range of localization for one dimensional random systems. *J. Phys. C* **1972**, *5*, 77–81. [CrossRef]

14. Ishii, K. Localization of eigenstates and transport phenomena in the one-dimensional disordered system. *Suppl. Progr. Theor. Phys.* **1973**, *53*, 77–138. [CrossRef]

15. Abou-Chacra, R.; Thouless, D.J. Self-consistent theory of localization. II. Localization near the band edges. *J. Phys. C* **1974**, *7*, 65–75. [CrossRef]

16. Thouless, D.J. Localisation in the Lloyd model. *J. Phys. C* **1983**, *16*, L929–L931. [CrossRef]

17. MacKinnon, A. Localisation in the Lloyd model of a disordered solid. *J. Phys. C* **1984**, *17*, L289–L291. [CrossRef]

18. Robbins, M.O.; Koiller, B. Localization properties of random and partially ordered one-dimensional systems. *Phys. Rev. B* **1985**, *32*, 4576–4583. [CrossRef]

19. Shepelyansky, D.L. Localization of quasienergy eigenfunctions in action space. *Phys. Rev. Lett.* **1986**, *56*, 677–680. [CrossRef]

20. Fishman, S.; Prange, R.E.; Griniasty, M. Scaling theory for the localization length of the kicked rotor. *Phys. Rev. A* **1989**, *39*, 1628–1633. [CrossRef]

21. Murdy, C.; Brouwer, P.W.; Halperin, B.I.; Gurarie, V.; Zee, A. Density of states in the non-Hermitian Lloyd model. *Phys. Rev. B* **1998**, *58*, 13539–13543. [CrossRef]

22. Deych, L.I.; Lisyansky, A.A.; Altshuler, B.L. Single parameter scaling in one-dimensional localization revisited. *Phys. Rev. Lett.* **2000**, *84*, 2678–2681. [CrossRef]

23. Deych, L.I.; Lisyansky, A.A.; Altshuler, B.L. Single-parameter scaling in one-dimensional Anderson localization: Exact analytical solution. *Phys. Rev. B* **2001**, *64*, 224202. [CrossRef]

24. Gangardt, D.M.; Fishman, S. Localization of eigenstates in a modified Tomonaga-Luttinger model. *Phys. Rev. B* **2001**, *63*, 045106. [CrossRef]

25. Fuchs, C.; Baltz, R.V. Optical properties of quantum wires: Disorder scattering in the Lloyd model. *Phys. Rev. B* **2001**, *63*, 085318. [CrossRef]

26. Titov, M.; Schomerus, H. Anomalous wave function statistics on a one-dimensional lattice with power-law disorder. *Phys. Rev. Lett.* **2003**, *91*, 176601. [CrossRef]

27. Mendez-Bermudez, J.A.; Martinez-Mendoza, A.J.; Gopar, V.A.; Varga, I. Lloyd-model generalization: Conductance fluctuations in one-dimensional disordered systems. *Phys. Rev. E* **2016**, *93*, 012135. [CrossRef]
28. Roy, D.; Kumar, N. Random-phase reservoir and a quantum resistor: The Lloyd model. *Phys. Rev. B* **2007**, *76*, 092202. [CrossRef]
29. Kozlov, G.G. Spectral dependence of the localization degree in the one-dimensional disordered Lloyd model. *Theor. Math. Phys.* **2012**, *171*, 531–540. [CrossRef]
30. Casati, G.; Guarneri, I.; Izrailev, F.M.; Fishman, S.; Molinari, L. Scaling of the information length in 1D tight-binding models. *J. Phys. Condens. Matter* **1992**, *4*, 149–156. [CrossRef]
31. Barthelemy, P.; Bertolotti, J.; Wiersma, D.S. A Levy flight for light. *Nature* **2008**, *453*, 495–498. [CrossRef]
32. Fernandez-Marin, A.A.; Mendez-Bermudez, J.A.; Carbonell, J.; Cervera, F.; Sanchez-Dehesa, J.; Gopar, V.A. Beyond anderson localization in 1D: Anomalous localization of microwaves in random waveguides. *Phys. Rev. Lett.* **2014**, *113*, 233901. [CrossRef]
33. Fernandez-Marin, A.A.; Mendez-Bermudez, J.A.; Carbonell, J.; Cervera, F.; Sanchez-Dehesa, J.; Gopar, V.A. Beyond Anderson localization: Anomalous transmission of waves through media with Levy disorder. In Proceedings of the 9th International Congress on Advanced Electromagnetic Materials in Microwaves and Optics (Metamaterials 2015), Oxford, UK, 7–12 September 2015; pp. 409–411.
34. Beenakker, C.W.J.; Groth, C.W.; Akhmerov, A.R. Nonalgebraic length dependence of transmission through a chain of barriers with a Levy spacing distribution. *Phys. Rev. B* **2009**, *79*, 024204. [CrossRef]
35. Burioni, R.; Caniparoli, L.; Vezzani, A. Levy walks and scaling in quenched disordered media. *Phys. Rev. E* **2010**, *81*, 060101(R). [CrossRef]
36. Eisfeld, A.; Vlaming, S.M.; Malyshev, V.A.; Knoester, J. Excitons in molecular aggregates with Levy-type disorder: Anomalous localization and exchange broadening of optical spectra. *Phys. Rev. Lett.* **2010**, *105*, 137402. [CrossRef]
37. Bertolotti, J.; Vynck, K.; Pattelli, L.; Barthelemy, P.; Lepri, S.; Wiersma, D.S. Engineering disorder in superdiffusive Levy glasses. *Adv. Funct. Mater.* **2010**, *20*, 965–968. [CrossRef]
38. Barthelemy, P.; Bertolotti, J.; Vynck, K.; Lepri, S.; Wiersma, D.S. Role of quenching on superdiffusive transport in two-dimensional random media. *Phys. Rev. E* **2010**, *82*, 011101. [CrossRef]
39. Burresi, M.; Radhalakshmi, V.; Savo, R.; Bertolotti, J.; Vynck, K.; Wiersma, D.S. Weak localization of light in superdiffusive random systems. *Phys. Rev. Lett.* **2012**, *108*, 110604. [CrossRef]
40. Groth, C.W.; Akhmerov, A.R.; Beenakker, C.W.J. Transmission probability through a Levy glass and comparison with a Levy walk. *Phys. Rev. E* **2012**, *85*, 021138. [CrossRef]
41. Burioni, R.; diSanto, S.; Lepri, S.; Vezzani, A. Scattering lengths and universality in superdiffusive Levy materials. *Phys. Rev. E* **2012**, *86*, 031125. [CrossRef]
42. Vlaming, S.M.; Malyshev, V.A.; Eisfeld, A.; Knoester, J. Subdiffusive exciton motion in systems with heavy-tailed disorder. *J. Chem. Phys.* **2013**, *138*, 214316. [CrossRef]
43. Burioni, R.; Ubaldi, E.; Vezzani, A. Superdiffusion and transport in two-dimensional systems with Levy-like quenched disorder. *Phys. Rev. E* **2014**, *89*, 022135. [CrossRef]
44. Bernabo, P.; Burioni, R.; Lepri, S.; Vezzani, A. Anomalous transmission and drifts in one-dimensional Levy structures. *Chaos Solitons Fractals* **2014**, *67*, 11–19. [CrossRef]
45. Zakeri, S.S.; Lepri, S.; Wiersma, D.S. Localization in one-dimensional chains with Levy-type disorder. *Phys. Rev. E* **2015**, *91*, 032112. [CrossRef]
46. Ardakani, A.G.; Nezhadhaghighi, M.G. Controlling Anderson localization in disordered heterostrctures with Levy-type distribution. *J. Opt.* **2015**, *17*, 105601. [CrossRef]
47. Falceto, F.; Gopar, V.A. Conductance through quantum wires with Levy-type disorder: Universal statistics in anomalous quantum transport. *Europhys. Lett.* **2010**, *92*, 57014. [CrossRef]
48. Fernandez-Marin, A.A.; Mendez-Bermudez, J.A.; Gopar, V.A. Photonic heterostructures with Levy-type disorder: Statistics of coherent transmission. *Phys. Rev. A* **2012**, *85*, 035803. [CrossRef]
49. Amanatidis, I.; Kleftogiannis, I.; Falceto, F.; Gopar, V.A. Conductance of one-dimensional quantum wires with anomalous electron wave-function localization. *Phys. Rev. B* **2012**, *85*, 235450. [CrossRef]
50. Amanatidis, I.; Kleftogiannis, I.; Falceto, F.; Gopar, V.A. Coherent wave transmission in quasi-one-dimensional systems with Lévy disorder. *Phys. Rev. E* **2017**, *96*, 062141. [CrossRef]
51. Anderson, P.W. Absence of diffusion in certain random lattices. *Phys. Rev.* **1958**, *109*, 1492–1505. [CrossRef]
52. Abrahams, E. (Ed.) *50 Years of Anderson Localization*; World Scientific, Singapore, Singapore, 2010.

53.	Anderson, P.W.; Thouless, D.J.; Abrahams, E.; Fisher, D.S. New method for a scaling theory of localization. *Phys. Rev. B* **1980**, *22*, 3519–3526. [CrossRef]

54.	Landauer, R. Spatial variation of currents and fields due to localized scatterers in metallic conduction. *IBM J. Res. Dev.* **1957**, *1*, 223–231. [CrossRef]

55.	Landauer, R. Spatial variation of currents and fields due to localized scatterers in metallic conduction. *IBM J. Res. Dev.* **1988**, *32*, 306–316. [CrossRef]

56.	Buttiker, M. Four-terminal phase-coherent conductance. *Phys. Rev. Lett.* **1986**, *57*, 1761–1764. [CrossRef]

57.	Buttiker, M. Symmetry of electrical conduction. *IBM J. Res. Dev.* **1988**, *32*, 317–334. [CrossRef]

58.	Lifshits, I.M.; Gredeskul, S.A.; Pastur, L.A. *Introduction to the Theory of Disordered Systems*; Willey: New York, NY, USA, 1988.

59.	Varga, I.; Pipek, J. Information length and localization in one dimension. *J. Phys. Condens. Matter* **1994**, *6*, L115–L122. [CrossRef]

60.	Mendez-Bermudez, J.A.; deOliveira, J.A.; Leonel, E.D. Two-dimensional nonlinear map characterized by tunable Levy fights. *Phys. Rev. E* **2014**, *90*, 042138.

61.	Mahaux, C.; Weidenmüller, H.A. *Shell Model Approach in Nuclear Reactions*; North-Holland Pub. Co.: Amsterdam, The Netherlands, 1969.

62.	Verbaarschot, J.J.M.; Weidenmüller, H.A.; Zirnbauer, M.R. Grassmann integration in stochastic quantum physics: The case of compound-nucleus scattering. *Phys. Rep.* **1985**, *129*, 367–438. [CrossRef]

63.	Rotter, I. A continuum shell model for the open quantum mechanical nuclear system. *Rep. Prog. Phys.* **1991**, *54*, 635–682. [CrossRef]

64.	Auerbach, N.; Zelevinsky, V. Super-radiant dynamics, doorways and resonances in nuclei and other open mesoscopic systems. *Rep. Prog. Phys.* **2011**, *74*, 106301. [CrossRef]

65.	Izrailev, F.M. Simple models of quantum chaos: Spectrum and eigenfunctions. *Phys. Rep.* **1990**, *196*, 299–392. [CrossRef]

66.	Metha, M.L. *Random Matrices*; Elsevier: Amsterdam, The Netherlands, 2004.

67.	Fyodorov, Y.F.; Mirlin, A.D. Analytical derivation of the scaling law for the inverse participation ratio in quasi-one-dimensional disordered systems. *Phys. Rev. Lett.* **1992**, *69*, 1093–1096. [CrossRef]

68.	Casati, G.; Molinari, L.; Izrailev, F.M. Scaling properties of band random matrices. *Phys. Rev. Lett.* **1990**, *64*, 1851–1854. [CrossRef]

69.	Evangelou, S.N.; Economou, E.N. Eigenvector statistics and multifractal scaling of band random matrices. *Phys. Lett. A* **1990**, *151*, 345–348. [CrossRef]

70.	Fyodorov, Y.F.; Mirlin, A.D. Scaling properties of localization in random band matrices: A σ-model approach. *Phys. Rev. Lett.* **1991**, *67*, 2405–2409. [CrossRef]

71.	Izrailev, F.M. Scaling properties of spectra and eigenfunctions for quantum dynamical and disordered systems. *Chaos Solitons Fractals* **1995**, *5*, 1219–1234. [CrossRef]

72.	Mirlin, A.D.; Fyodorov, Y.F. The statistics of eigenvector components of random band matrices: Analytical results. *J. Phys. A Math. Gen.* **1993**, *26*, L551–L558. [CrossRef]

73.	Fyodorov, Y.F.; Mirlin, A.D. Level-to-level fluctuations of the inverse participation ratio in finite quasi 1D disordered systems. *Phys. Rev. Lett.* **1993**, *71*, 412–415. [CrossRef]

74.	Fyodorov, Y.F.; Mirlin, A.D. Statistical properties of eigenfunctions of random quasi 1D one-particle Hamiltonians. *Int. J. Mod. Phys. B* **1994**, *8*, 3795–3842. [CrossRef]

75.	Casati, G.; Guarneri, I.; Izrailev, F.M.; Scharf, R. Scaling behavior of localization in quantum chaos. *Phys. Rev. Lett.* **1990**, *64*, 5–8. [CrossRef]

76.	Mendez-Bermudez, J.A.; Ferraz de Arruda, G.; Rodrigues, F.A.; Moreno, Y. Diluted banded random matrices: scaling behavior of eigenfunction and spectral properties. *J. Phys. A Math. Theor.* **2017**, *50*, 495205. [CrossRef]

77.	Mendez-Bermudez, J.A.; Ferraz de Arruda, G.; Rodrigues, F.A.; Moreno, Y. Scaling properties of multilayer random networks. *Phys. Rev. E* **2017**, *96*, 012307. [CrossRef]